

# **Powder Characteristics, Microstructure and Properties of Graphite Platelet Reinforced Poly Ether Ether Ketone composites in High Temperature Laser Sintering**

Yuan Wang <sup>a\*</sup>, Davood Rouholamin <sup>a</sup>, Richard Davies <sup>b</sup> Oana R. Ghita <sup>a</sup>

<sup>a</sup> University of Exeter, Department of Engineering, Mathematics and Physical Sciences, North Park Road, EX4 4QF, UK

<sup>b</sup> Centre for Additive Layer Manufacturing (CALM), University of Exeter, Department of Engineering, Mathematics and Physical Sciences, North Park Road, EX4 4QF, UK

\*Corresponding author: [y.wang@ex.ac.uk](mailto:y.wang@ex.ac.uk) Tel: +44-1392-725779

## **Abstract**

The properties of graphite platelet reinforced Poly Ether Ether Ketone (PEEK/GP) composites from powder to laser sintered parts were investigated in this study. The flowability, particle size and laser absorption characteristics of PEEK/GP powders with various graphite loadings were studied. It was found that the addition of graphite improved laser absorption; however, the flowability of powder was reduced. Micro-CT scanning was used to study the distribution, dispersion and the orientation of graphite platelets as well as the porosity and maximum pore size of laser sintered PEEK/GP composites. The graphite platelets were observed to be distributed evenly in the structure without significant agglomeration. Most of the graphite had their in-plane surface orientated in the X-Y plane of fabrication, which increased the tensile strength of the composites incorporating 5wt% graphite. The investigation also demonstrated that the porosity and maximum pore size increased with increasing amounts of graphite. A significant increase in porosity and pore size was found in PEEK/GP composites with 7.5wt% graphite, and it is believed to be responsible for the drop in tensile strength. DMA analysis showed no reduction of the damping properties in the composites incorporating up to 5wt% graphite, whereas the composites with 7.5wt% graphite showed increased stiffness.

**Keywords:** Laser Sintering, PEEK, Composites, Thermomechanical properties, Micro-CT, Microstructure characterization.

## 1. Introduction

PolyEtherEtherKetones (PEEK) are used in many industry sectors as thermal insulators due to their high melting temperature ( $>300\text{ }^{\circ}\text{C}$ ), as medical implants due to the material's biocompatibility and as bearing parts in pumps due to their good wear and chemical resistance.[1,2,3] PEEK is also often used as a composite material with other additives, and reinforcements to further increase its mechanical or thermal performance. [4,5] In traditional manufacturing, PEEK has been reinforced with various types of carbon structures including carbon fibre, graphite and carbon nanotubes (CNTs) [6,7,8]. Depending on the application, the objective was an improvement of prolonged fatigue stress and strain characteristics [9], strength or thermal and electrical performance [10]. The freedom of design offered by the techniques available within additive manufacturing (AM) also triggered interest in the use of high temperature polymers and their composites for use in medical and aerospace applications. Unfortunately, the standard laser sintering process was limited to the use of nylon as the most widely used and best performing engineering polymer. For a long time, the improvement in performance was sought through the incorporation of reinforcement rather than improvement of performance of the polymer matrices.

Several methods for developing composites by Selective Laser Sintering (SLS) have been reported. Goodridge et al., compounded PA12 with 3% by weight carbon nanofibers (CNF) followed by mechanical cryogenic milling and found a 22% increase in storage modulus. [11] Although the particle morphology was not extensively investigated, the authors reported a rough surface finish of SLS composite parts due to the angular shaped powder produced by mechanical milling. Karevan et al., reported a wet coating method to produce PA12/exfoliated Graphite nanoPlatelets (GnP) for laser sintering [12]. They found an increase in tensile modulus and slight decrease in flexural modulus with 3% GnP added by

weight. Composite fabricated with 5% GnP presented a lower strength compared with those incorporating 3% GnP due to agglomeration of the nanofiller. Bai et al., [13] used a patented chemical method [14] to create PA12 particles surface coated with CNTs and reported a 44.5% increase in tensile modulus and 7% increase in tensile strength for 0.1wt% CNTs [10, 11].

The addition of carbon type reinforcement in nylon polymeric powder offered some degree of improvement in mechanical performance but it did not overcome the intrinsic limitation of low glass transition temperature of the matrix, which ultimately restricts use of nylon or nylon composite materials in harsh environments with high operating temperature such as aerospace, defence, marine or petrol and gas applications. The introduction to the AM market of the commercial high temperature laser sintering system, the EOSINT P800, allowed this drawback to be addressed. This system is currently available with the commercial laser sintering grade Poly Ether Ketone (PEK) HP3 powder [15, 16, 17], and recently researched and tested Victrex PEEK 450PF powder. [18] Prior to the EOSINT P800 system and the two grades currently available, there were several attempts to laser sinter PEEK in modified standard systems. In most cases, the focus was on machine modifications and process parameters rather than properties of sintered parts. Wagner et al., mixed PEEK with up to 0.15% carbon black powder by intensive shaking procedures and sintered only single layer specimens with a modified YAG laser system at room temperature [19]. The study demonstrated that small amounts of carbon black, less than 1wt%, significantly improved the laser absorption and powder bed temperature. The authors concluded that the laser energy is initially absorbed by carbon black particles followed by energy transfer from carbon black particles to the surrounding polymer powder, facilitating the sintering. Rechtenwald et al., [20] modified an EOSINT P380 laser sintering machine by integrating a circular building platform and an additional heating device to enable pre-heating at higher temperatures (250 °C). Following on from this study, researchers within the same group [21] tried to further improve

the modified system by adding a “high-temperature inner process chamber” called the “Heating Dome” to the standard PA12 equipment and manufactured PEEK/ tricalcium phosphate and PEEK/carbon black composite for medical applications [22]. However, the mechanical properties of these composites were not studied.

PEEK and PEK belong to the same family of high temperature polymers and have similar performance but different melting and glass transition temperatures. PEEK is preferred for manufacturing as it has a lower processing temperature compared with PEK, which subsequently reduces any degradation effects and potentially uses less processing energy. PEK HP3 powder has been commercially available as a laser sintering grade for the last few years [23], where Victrex PEEK 450PF has just recently appeared as the next high temperature polymeric powder suitable for laser sintering. [18] This paper continues the investigation into PEEK and HT-LS, by analysing the feasibility of manufacturing PEEK/graphite composites using the EOSINT P800 system. The current study presents for the first time properties of PEEK/graphite powder and sintered composites. Small amount of graphite up to 5% wt improved the mechanical strength of the composites, whereas incorporating of 7.5% wt graphite leads to the drop in tensile strength. The micro-CT results provide evidence for the drop in strength noticed at 7.5%wt graphite loadings.

## **2. Experimental**

### *2.1 Materials preparation*

The powder used for fabrication was PEEK150PF powder supplied by Victrex plc with an average particle size of 60µm. Graphite platelets were supplied by Easy Composites.

According to the manufacture’s specification, 85% of the graphite powder has a particle size less than 44µm. PEEK powder was thermally treated in an oven at 250°C for 24hrs before dry

mixing. The PEEK/ graphite platelets at weight ratios of 99/1, 95/5 and 92.5/7.5 were then mixed manually in a drum until the mixture achieved a uniform colour. Then, further mixing was carried out by rolling the drum on an EOS electric powder mixer for 2 hours. The mixed powder was sieved using an EOS powder sieve with a 245 $\mu$ m mesh screen and used for laser sintering.

## *2.2 Fabrication of PEEK/GP by HT-LS*

The high temperature laser sintering (HT-LS) process was carried out in a reduced build mode using the EOSINT P800 system. Descriptions of the build chamber modes and the PEEK processing parameters are available in previous publications [18]. Tensile specimens and rectangular bars were built according to ISO527-2 test specimen type A1 and B1, respectively. Rectangular samples were used for DMA specimens. To allow understanding of any potential variation in properties of parts related with position of specimens in the build chamber, the samples build set up is shown in Figure 1.

## *2.3 Characterisation of powder*

### *2.3.1 FTIR analysis*

A Bruker Matrix FTIR was used to determine the absorbance values of the PEEK/GP dry mixed powder at a wavelength of 943 $\text{cm}^{-1}$ , which is equal to the wavelength of the CO<sub>2</sub> laser beam equipped on the high temperature laser sintering equipment.

### *2.3.2 Angle of repose*

The angle of repose test was used to check the powder flowability. The experiment was performed at room temperature as according to ASTM C144. The powder was poured onto a horizontal surface through a funnel to form a cone. The nozzle tip of the funnel was placed at a height of 38.1 mm from the flat surface. Feeding was stopped when the cone reached the tip

of the funnel nozzle. Then the diameter of the cone was measured in 4 positions and the angle of repose (AOR) was calculated by equations (1) and (2):

$$AOR = \tan^{-1} 2 * (H/Da) \quad (1)$$

$$Da = \sum Di/4 \quad (2)$$

Where  $H$  is the height of the cone (=38.1 mm),  $D_a$  is average of the 4 diameters and  $D_i$  is the measured diameter. Six repeats were carried out for each type of powder.

### *2.3.3 Particle size distribution*

To measure the particle size distribution, the particles were dispersed in deionized water to form suspensions. Then the suspensions were tested with a Saturn DigiSizer 5200 Micrometrics to obtain the particle size distribution.

### *2.4 SEM Characterisation*

Microstructure analysis of the PEEK powder, graphite powder and the fractured surface of composite samples was carried out by secondary electron microscopy (SEM) (Hitachi S-3200N, Japan). The secondary electron images were taken under 25 kV accelerating voltages.

### *2.5 Micro-CT*

Micro-CT was used in this study to investigate the 3D structure of the laser sintered parts. The mechanism of micro-CT is described in a study by Ho and Hutmacher.[24] Cubic-shaped samples were cut carefully from the laser sintered tensile test specimens of PEEK and PEEK composite with 1, 5 and 7.5 wt% GP. These micro-CT samples had dimensions of approximately  $3 \times 3 \times 3$  mm. As indicated in Figure 2, the micro-CT samples were cut from the centre part of the tensile test specimens which were built according to the ISO standard ISO527-2. The Micro-CT samples were mounted in the CT machine in the same orientation as during the sintering process. The prepared samples were scanned using X-Tek Bench top

CT 160 Xi (X-Tek Systems Ltd/Nikon Metrology UK Ltd, England) with a current of 95-100  $\mu\text{A}$ , voltage of 65-70 kV, pixel size of 3  $\mu\text{m}$  and 360° rotation. According to the mechanism of micro-CT scanning, each specimen is virtually divided into a series of 2D slices that are irradiated with X-rays. The CT data produced from scanning was then analysed using VGStudio MAX software. Morphological characteristics such as porosity, maximum pore size and maximum graphite size were measured, and orientation of the graphite in the 3D reconstruction of the PEEK was investigated. Three samples were scanned for each composition, and three regions of interest were selected for each sample for the porosity measurements. Hence, the porosity was measured for nine samples for each composition. The maximum pore size and maximum graphite size in the specimens were measured by analysing all the 2D images produced from the CT scanning from various depths of the structure. The sizes of the largest pores and largest graphite platelets were recorded. 22 measurements were noted for each composition, and the maximum values for the two parameters were then obtained from these measurements.

### *2.6 Mechanical testing*

The tensile tests were performed on a Lloyds EZ20 machine with a crosshead speed of 2mm/min for all samples. Ten specimens for each material were tested. The dimensions of the tensile testing specimens are presented in Figure 2.

### *2.7 Dynamic mechanical thermal analysis (DMTA)*

DMTA specimens with dimension of 30 x 7 x 2 mm were milled from rectangular samples. The dynamic mechanical tests were performed on a Mettler Toledo DMA1 STARe system using the temperature scanning mode with a three-point bending sample supporting jig. The length of the supporting span was 20 mm. The temperature range was 40-280°C with a

heating rate of  $3 \text{ K min}^{-1}$ . Tests were performed with a frequency of 1Hz and a controlled displacement amplitude of  $10\mu\text{m}$ . Storage modulus ( $E'$ ), loss modulus ( $E''$ ) and the damping factor ( $\tan \delta$ ) were obtained from DMTA testing.

### 3 Results and Discussion

#### 3.1 FTIR analysis

The FTIR absorbance and reflectance of pure PEEK, graphite and PEEK/graphite composites are shown in Figure 3 (a). The graphite platelets show significantly higher absorbance of light than PEEK150PF powder. The absorption increased with increasing amounts of graphite, except for the addition of 1% graphite, which was not observed to affect the optical properties, as its absorbance values remained similar to those of pure PEEK powder.

#### 3.2 Characterisation of powder

A good powder for laser sintering needs to flow well to spread smoothly and to achieve dense powder compaction. Table 1 presents the AOR data of various powders. Commercial laser sintering grade PEK HP3 is studied as a benchmark material. Though the PEEK 150PF powder showed less flowability than PEK HP3, it dispersed well during powder spreading. It can also be seen from the AOR data that graphite platelets reduced the flowability of the composite powder.

	PEK HP3	PEEK 150PF	PEEK/1%GP	PEEK/5%GP	PEEK/7.5%GP	GP
AOR	$37.8\pm 0.4$	$40.5\pm 0.3$	$43.6\pm 0.3$	$45.3\pm 0.2$	$46.1\pm 0.2$	$50.2\pm 0.2$

Table 1: The AOR of various powders

The particle size distributions of PEK, PEEK and graphite platelets are shown in Figure 3(b). The PEEK powder has similar particle size distribution compared with the laser sintering PEK grade. The average particle size is approximately  $60\mu\text{m}$ . The graphite platelets have a

broader particle size distribution than the polymer powder with average particle size of approximately 30 $\mu\text{m}$ .

### *3.3 SEM Characterisation*

Figure 4(a) and (b) show the morphology of PEK and PEEK, respectively. The morphology of the graphite platelets used for fabrication of the composite is shown in Figure 4(c) and (d). The PEEK particles have elongated shapes and their surface is rougher compared with the commercial PEK grade. The morphology of the two powders, PEK and PEEK, was presented in more detail in a previous publication by the same group. [25] Figures 4(e)-(g) show the morphology of the mixed composite powder; the PEEK particles are predominantly coated by the small graphite platelets having size less than 30 $\mu\text{m}$ . As demonstrated with the FTIR absorption at 943 $\text{cm}^{-1}$  (Figure 3), these graphite platelets could effectively improve the laser absorption and transfer of heat to the PEEK particles.

Figure 5 shows the fracture surface of PEEK and PEEK/GP composite parts with various GP loadings fabricated by high temperature laser sintering (HT-LS). The pure PEEK shows an anisotropic layered structure. This has been frequently noticed in laser-sintered structures, it is an inherent characteristic of the additive manufacturing process, which can be reduced by changing processing conditions, but not totally eliminated. This microstructure was noticed also in the previous HT-LS PEEK papers [16, 17, 26,] As a result of the layered structure, the laser sintered materials showed anisotropic tensile strength in X, Y and Z directions [27, 28]. The layered structure seems to disappear in the PEEK/GP composites as seen in Figure 5 (b), (c) and (d). This result implies that the addition of graphite improved the fusion between layers as a result of enhanced heat absorption. The fracture surfaces of the PEEK/GP composites shown in Figure 6 reveal the presence of some graphite platelets partially pulled

out of the matrix. It can be seen that their out-of-plane surface is almost perpendicular to the fracture surface. Graphite orientation in the laser sintered samples was studied by Micro-CT and the influence of their orientation on mechanical performance is discussed in the following sections.

### *3.4 Micro-CT*

Micro-CT was employed to investigate the 3D structure of the laser sintered parts in terms of the distribution, dispersion and orientation of graphite platelets, porosity and maximum pore size in the samples. The 3D reconstruction image is sliced into 2D images through x, y, and z directions (as indicated in Figure 7(a)) to investigate the distribution of the graphite platelets. Figure 7(a) demonstrates the 3D reconstruction of a PEEK sample with 7.5wt% graphite and Figures 7(b) to (d) show the sliced 2D images in z direction of pure PEEK and PEEK composites with 1, 5 and 7.5wt% graphite loadings. During the CT scanning, a higher intensity of X-ray is reflected and collected for the areas or particles with higher density, and therefore these areas can be observed as white or bright colour in the images. [36] The black areas in the 2D images represent the pores in the structure, and the bright areas represent the denser part of the structure, such as graphite. The pores and graphite in the structures are highlighted in the images. As demonstrated, it was found that the graphite was uniformly distributed throughout the structure for each type of sintered composite. Figure 7 also suggests that the porosity and pore size increase as the amount of graphite in the structure increases. It was also noticed that the porosity and pore size seem to increase significantly when the graphite in the PEEK structure increases from 5% to 7.5wt% GP. Figure 8 shows the sliced 2D image and 3D reconstructions of scanned PEEK/5% GP and PEEK/7.5% GP samples. It shows that the PEEK/7.5% GP sample possesses a visibly higher porosity with larger pores in the structure compared to the PEEK/5% GP sample.

In order to quantify the maximum pore size and dispersion of graphite in the composites, the pore size and graphite size in each sliced 2D image were measured to determine the maximum value. The measured porosity, maximum pore size and maximum graphite size from micro-CT are presented in Table 2.

Graphite (%)	Porosity (%)	Maximum pore size ( $\mu\text{m}$ )	Maximum graphite size ( $\mu\text{m}$ )
0	$7.4 \pm 0.1$	$40.6 \pm 5.2$	---
1	$9.4 \pm 1.4$	$89.4 \pm 13.2$	$121.2 \pm 14.3$
5	$12.9 \pm 1.1$	$179.4 \pm 31.5$	$157.5 \pm 17.2$
7.5	$27.9 \pm 1.6$	$305.7 \pm 37.9$	$140.5 \pm 14.4$

Table 2: Porosity, maximum pore size and maximum graphite size of the structures with various percentages of graphite measured by micro-CT.

As platelets, the in-plane surface of graphite is larger than the out of plane surface. By comparing the 2D images sliced through z direction in Figure 8 (top left corner) to the images sliced along x and y directions (top right and bottom left corners respectively), it can be observed that the in-plane surface of graphite lay on the x-y plane of Micro-CT image which is same as the X-Y plane of fabrication. The same graphite orientation was observed in the majority of sliced 2D images of all PEEK/GP composites. As presented in Table 2, the quantified results of porosity are consistent with the SEM image analysis and show that the sintered pure PEEK structure has the lowest porosity which gradually increases with the increase of graphite loading. There was a significant increase in porosity from 13% to 28% when the amount of graphite was increased from 5% to 7.5%. As shown by the FTIR test, the graphite will absorb more laser energy, allowing a higher temperature to be attained in the LS system. The presence of more pores in the sintered composite structure could be due to uneven energy absorption across the deposit layer. The regions where graphite is present will absorb more energy and have a higher degree of melting and flow, whereas regions without graphite will absorb less energy and therefore have less flow. This effect is combined with

the fact that the PEEK powder particles have a different morphology to the commercial grade PEK HP3. The PEEK particles are less round, have an elongated shape and sometimes fibrils which make the sintering of pure PEEK itself less uniform, and when combined with a non-uniform energy distribution will lead to creation of more pores in the structure. [25] A recent study by Berretta et al., confirmed this cavity formation mechanism in each powder layer as a result of powder morphology. [18] In addition, graphite and PEEK materials have significantly different thermal conductivities ( $0.32 \text{ Wm}^{-1} \text{ K}^{-1}$  for Victrex PEEK 450G [29],  $140\text{-}500 \text{ Wm}^{-1} \text{ K}^{-1}$  for in plane graphite sheet and  $3\text{-}10 \text{ Wm}^{-1} \text{ K}^{-1}$  out of plane graphite sheet [30,31]) which means that the two components absorb and dissipate heat differently. The heat transfer and thermal equilibrium might not be fully achieved for each layer deposition and sintering. Another reason for the increased porosity measurements noticed in composites at 7.5% graphite loadings could be related with the reduced flowability of the composite powder as shown by the AOR data, which may lead to difficulty in achieving uniform powder spreading and enhance the probability of having porosity in the sintered structure. Quantitative analysis also showed that there is no significant change in the maximum graphite size as the percentage of graphite in the structure increases (Table 1), which is in agreement with the micro-CT images. The maximum size of graphite measured in all composites from the micro-CT images is larger than that measured by the particle analyser. This could be due to a small degree of agglomeration of graphite platelets in the composites.

### *3.5 Mechanical performance*

Figure 9 shows that the addition of 1% and 5% GP (by weight) led to 15 % and 36 % increase in tensile strength, respectively. However, a further increase in the percentage of graphite platelets to 7.5 % led to a reduction in tensile strength. PEEK/7.5%GP composite shows less strength improvement effect compared with those with 1% and 5wt% graphite content. It can

also be seen that the strain% increases with increasing graphite content; PEEK/5% GP shows an increase in tensile strain% of approximately 40%. The study carried out by Ho et al., [32] clearly showed, through a combination of graphite and polycarbonate single layer tests, that the addition of graphite platelets greatly promotes the laser absorption, increases the temperature of the powder bed, and improves the fusion of the polymer powder. A better fusion of the polymeric powder is expected to lead to parts with higher strength. Such a trend was noticed here for 1% and 5% GP; followed by a significant drop at 7.5% graphite platelets. Yasmin and Daniel [33], Agag et al., [34] and Karevan et al. [35] reported similar effects. Karevan et al., recorded an increase in tensile strength for laser sintered nylon samples with 3% exfoliated GnP, followed by a decrease in strength values for samples incorporating 5% of the same nanoplatelets. Agglomeration of the reinforcement particles was assumed to be the factor responsible for the drop in strength in all referenced studies. However, in our case, the agglomeration of graphite platelets was not responsible for reduced mechanical performance. As shown in micro-CT images, the graphite platelets were well dispersed throughout all samples. The micro-CT data revealed an increase in the porosity and pore size within the composite structure with increasing graphite platelet content, especially for 7.5% graphite platelets loading. As previously mentioned, the porosity was associated with the powder morphology, its poor flowability and laser energy absorption during sintering. Although the presence of pores in sintered parts can lead to lower mechanical performance of the parts [36, 37, 38], PEEK/GP composites showed improved tensile strength compared with virgin PEEK, despite the porosity. This implies the graphite platelets act as reinforcement in the direction of the tensile testing and overall may have a positive effect on the strength of the composite. During tensile test, these aligned graphite platelets may delay the crack propagation. The crack will travel a longer path around the polymer/graphite interface rather than straight through a pure PEEK matrix. The incorporation of the graphite may have changed the crystal

structure of the matrix and changed the deformation behaviour, for example, increasing the % strain as shown in Figure 9(b). The review by Diez-Pascual et al discussed unusual melting and crystallization behaviour of PEEK and PEK with carbon fibres (Cf), carbon nano-fibres (Cnf) and graphite and found an increase in % strain for certain combinations and conditions of matrix and reinforcement. [39]

### *3.6 Thermo-mechanical performance*

Figure 10 shows the damping factor  $\tan \delta$ , storage modulus ( $E'$ ) and loss modulus ( $E''$ ) of PEEK and PEEK/GP composites with 1%, 5%, 7.5% graphite loadings. The  $E'$  and  $E''$  were found to increase in value with the increase of graphite platelet content. Addition of 1% and 5% graphite has no influence on the damping peak maximum of PEEK and its location, which is associated with  $T_g$ . Similar results were reported by Karevan et al.[35] who demonstrated that the addition of a small amount of graphite nanoplates had no effect on the  $T_g$  of laser sintered PA12 composites. In our study, the incorporation of 7.5% graphite platelets led to an increase in  $T_g$  of approximately 10°C and a slight decrease in the damping factor,  $\tan \delta$ , which indicates an increase in the rigidity of the structure. The DMA results here have a similar behaviour to those observed in several previous studies which showed that the incorporation of rigid filler into polymer immobilizes the motion of polymer chains as a result of interface interaction between filler and polymer. [40, 41, 42].

## **4 Conclusion**

Microstructure and mechanical behaviour of laser sintered PEEK/GP composites were studied. The Micro-CT study demonstrated that the graphite was well distributed in all composites with no obvious agglomeration throughout their structure, but revealed an increase in porosity and maximum pore size in the composite with increasing loading of

graphite. It is believed that the pores were the results of a poor powder morphology, which led to lower flowability (shown by the AOR data) and uneven laser energy absorption. Despite the porosity, the in-plane graphite platelets aligned along the X-Y plane of sintering and reinforced the tensile strength of the composites. PEEK/5%GP composite had the highest strength improvement, 36%, compared to other samples. The graphite orientation also led to an increase in tensile strain %. Incorporation of 7.5 wt% GP resulted in a 40 % increase in strain %. The DMA analysis demonstrated that the graphite improved the modulus of the PEEK composite. The results clearly demonstrated the importance of powder morphology and powder preparation in laser sintering and its influence on the mechanical performance of the composite.

## Reference

- 
- [1] Attwood TE, Dawson PC, Freeman JL, Hoy LRJ, Rose JB, Staniland PA. Synthesis and properties of polyaryletherketones. *Polymer*. 1981;22(8):1096-103.
- [2] Kurtz SM, Devine JN. PEEK biomaterials in trauma, orthopedic, and spinal implants. *Biomaterials*. 2007;28(32):4845-69.
- [3] Jones DP, Leach DC, Moore DR. Mechanical properties of poly(ether-ether-ketone) for engineering applications. *Polymer*. 1985;26(9):1385-93.
- [4] Wu G-M, Schultz JM., Processing, microstructure, and failure behavior in short-fiber-reinforced poly(ether ether ketone) composites. *Polymer Composites*. 1990;11(2):126-32.
- [5] Voss H, Friedrich K. On the wear behaviour of short-fibre-reinforced PEEK composites. *Wear*. 1987;116(1):1-18.
- [6] Gao S-L, Kim J-K., Cooling rate influences in carbon fibre/PEEK composites. Part 1. Crystallinity and interface adhesion. *Composites Part A: Applied Science and Manufacturing*. 2000;31(6):517-30.
- [7] Tripathy BS, Furey MJ. Tribological behavior of unidirectional graphite-epoxy and carbon-PEEK composites. *Wear*. 1993;162–164, Part A(0):385-96.

- 
- [8] Díez-Pascual AM, Naffakh M, González-Domínguez JM, Ansón A, Martínez-Rubi Y, Martínez MT, High performance PEEK/carbon nanotube composites compatibilized with polysulfones-II. Mechanical and electrical properties. *Carbon*. 2010;48(12):3500-11.
- [9] Steinberg EL, Rath E, Shlaifer A, Chechik O, Maman E, Salai M. Carbon fiber reinforced PEEK Optima—A composite material biomechanical properties and wear/debris characteristics of CF-PEEK composites for orthopedic trauma implants. *Journal of the Mechanical Behavior of Biomedical Materials*. 2013;17(0):221-8.
- [10] Díez-Pascual AM, Ashrafi B, Naffakh M, González-Domínguez JM, Johnston A, Simard B, Influence of carbon nanotubes on the thermal, electrical and mechanical properties of poly(ether ether ketone)/glass fiber laminates. *Carbon*. 2011; 49 (8): 2817-33.
- [11] Goodridge RD, Shofner ML, Hague RJM, McClelland M, Schlea MR, Johnson RB, et al. Processing of a Polyamide-12/carbon nanofibre composite by laser sintering. *Polymer Testing*. 2011;30(1):94-100.
- [12] Athreya SR, Kalaitzidou K, Das S. Mechanical and microstructural properties of Nylon-12/carbon black composites: Selective laser sintering versus melt compounding and injection molding. *Composites Science and Technology*. 2011;71(4):506-10.
- [13] Bai J, Goodridge RD, Hague RJM, Song M. Improving the mechanical properties of laser-sintered polyamide 12 through incorporation of carbon nanotubes. *Polymer Engineering & Science*. 2013;53(9):1937-46.
- [14] Cai D, Jin J and Song M. Process. UK Patent WO/2009/034361, 2009.
- [15] Ghita OR, James E, Trimble R, Evans KE. Physico-chemical behaviour of Poly (Ether Ketone) (PEK) in High Temperature Laser Sintering (HT-LS), *Journal of Materials Processing Technology*. 2014; 214(4): 969-978,
- [16] Ajoku U, Saleh N, Hopkinson N, Hague R, Erasenthiran P. Investigating mechanical anisotropy and end-of-vector effect in laser-sintered nylon parts. *Proceedings of the Institution of Mechanical Engineers, Part B: Journal of Engineering Manufacture*. 2006;220(7):1077-86.
- [17] Wang Y, James E, Ghita OR. Glass bead filled Polyetherketone (PEK) composite by High Temperature Laser Sintering (HT-LS), *Materials & Design*, 2015;83:545-51.
- [18] Berretta S, Evans KE, Ghita OR. Processability of PEEK, a new polymer for High Temperature Laser Sintering (HT-LS), *European Polymer Journal*.2015;68:243-66.

- 
- [19] Wagner T, Höfer T, Knies S, Eyerer P. Laser Sintering of High Temperature Resistant Polymers with Carbon Black Additives. *International Polymer Processing*. 2004;19(4):395-401.
- [20] Rechtenwald T, Eßer G, Schmidt M, Pohle D, Comparison between Laser Sintering of PEEK and PA using Design of Experiment Methods, *Lasers in Manufacturing 2005*. Munich(Germany): Proceedings of the 3rd International WLT-Conference on Lasers in Manufacturing, 2005; p. 263–7.
- [21] Schmidt M, Pohle D, Rechtenwald T. Selective Laser Sintering of PEEK. *CIRP Annals - Manufacturing Technology*. 2007;56(1):205-8.
- [22] Pohle D, Ponader S, Rechtenwald T, Schmidt M, Schlegel KA, Münstedt H, et al. Processing of Three-Dimensional Laser Sintered Polyetheretherketone Composites and Testing of Osteoblast Proliferation in vitro. *Macromolecular Symposia*. 2007;253(1):65-70.
- [23] EOS materials data sheet: <http://eos.materialdatacenter.com/eo/en>
- [24] S.T. Ho and D.W. Hutmacher, A comparison of micro CT with other techniques used in the characterization of scaffolds. *Biomaterials* 2006; 27(8): 1362-1376.
- [25] Berretta S, Ghita O, Evans KE. Morphology of polymeric powders in Laser Sintering (LS): From Polyamide to new PEEK powders. *European Polymer Journal*. 2014;59(0):218-29.
- [26] Beard MA, Ghita OR, Bradbury J, Flint S, Evans KE. Material characterisation of additive manufacturing components made from a polyetherketone (PEK) high temperature thermoplastic polymer. 5<sup>th</sup> International Conference on Advanced Research in Virtual and Rapid Prototyping. Leiria (Portugal): Innovative Developments in Virtual and Physical Prototyping, 2011;329-32.
- [27] Ghita O, James E, Davies R, Berretta S, Singh B, Flint S, Evans E., High Temperature Laser Sintering (HT-LS): An investigation into mechanical properties and shrinkage characteristics of Poly (Ether Ketone) (PEK) structures. *Materials & Design*. 2014;61(0):124-32.
- [28] Gibson I, Shi D. Material properties and fabrication parameters in selective laser sintering process. *Rapid Prototyping Journal*. 1997;3(4):129-36.
- [29] Victrex materials datasheet: <http://www.victrex.com/en/victrex-peek>
- [30] Kang. S, Cook. R, Gailus. D, Testing the thermal resistance and power capacity of production heat pipe, Proceedings of IPACK2005 ASME. 2005; 635-640.

- 
- [31] Smalc. M, Shives. G, Chen. G, Guggari. S, Norley. J and Reynolds. R. A, Thermal Performance of Natural Graphite Heat Spreaders, Proceedings of IPACK2005 ASME. 2005: 79-89.
- [32] Ho HCH, Cheung WL, Gibson I. Effects of graphite powder on the laser sintering behaviour of polycarbonate. Rapid Prototyping Journal. 2002;8(4):233-42.
- [33] Yasmin A, Daniel IM. Mechanical and thermal properties of graphite platelet/epoxy composites. Polymer. 2004;45(24):8211-9.
- [34] Agag T, Koga T, Takeichi T. Studies on thermal and mechanical properties of polyimide–clay nanocomposites. Polymer. 2001;42(8):3399-408.
- [35] Karevan M, Eshraghi S, Gerhardt R, Das S, Kalaitzidou K. Effect of processing method on the properties of multifunctional exfoliated graphite nanoplatelets/polyamide 12 composites. Carbon. 2013;64(0):122-31.
- [36] Rouholamin D, Hopkinson N. An investigation on the suitability of micro-computed tomography as a non-destructive technique to assess the morphology of laser sintered nylon 12 parts. Proceedings of the Institution of Mechanical Engineers, Part B: Journal of Engineering Manufacture. 2014;228(12):1529-42.
- [37] Hopkinson N, Majewski CE, Zarringhalam H. Quantifying the degree of particle melt in Selective Laser Sintering®. CIRP Annals - Manufacturing Technology. 2009;58(1):197-200.
- [38] H. Zarringhalam and N. Hopkinson, Post-processing of Duraform™ parts for rapid manufacture, 14<sup>th</sup> solid freeform fabrication (SFF) symposium. University of Texas(Austin): Proceedings of the 14th solid freeform fabrication (SFF) symposium, 2003; p596-606.
- [39] Díez-Pascual AM, Naffakh M, Marco C, Ellis G, Gómez-Fatou MA. High-performance nanocomposites based on polyetherketones. Progress in Materials Science. 2012;57(7):1106-90.
- [40] Russo P, Acierno D, Rosa R, Leonelli C, Corradi A, Rizzuti A. Mechanical and dynamic-mechanical behavior and morphology of polystyrene/perovskite composites: Effects of filler size. Surface and Coatings Technology. 2014;243(0):65-70.
- [41] d’Almeida JRM, Monteiro SN, Menezes GW, Rodriguez RJS. Diamond-Epoxy Composites. Journal of Reinforced Plastics and Composites. 2007;26(3):321-30.
- [42] Manikandan Nair KC, Thomas S, Groeninckx G. Thermal and dynamic mechanical analysis of polystyrene composites reinforced with short sisal fibres. Composites Science and Technology. 2001;61(16):2519-29.

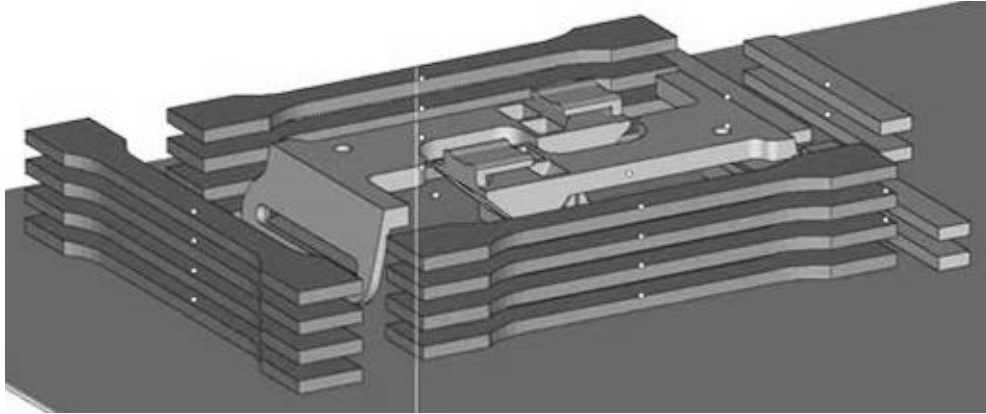


Figure 1: Build positions of PEEK/GP composite samples. Dog bone and rectangular samples are manufactured for tensile testing and DMA tests respectively. The two samples located in the middle of the build were manufactured for demonstration purposes. They were designed for an aerospace application.

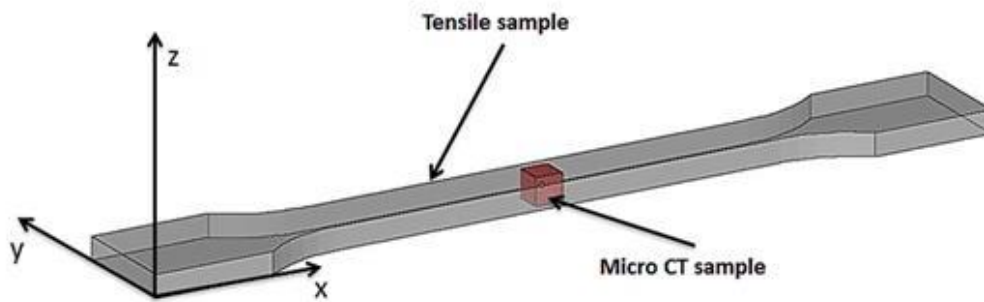
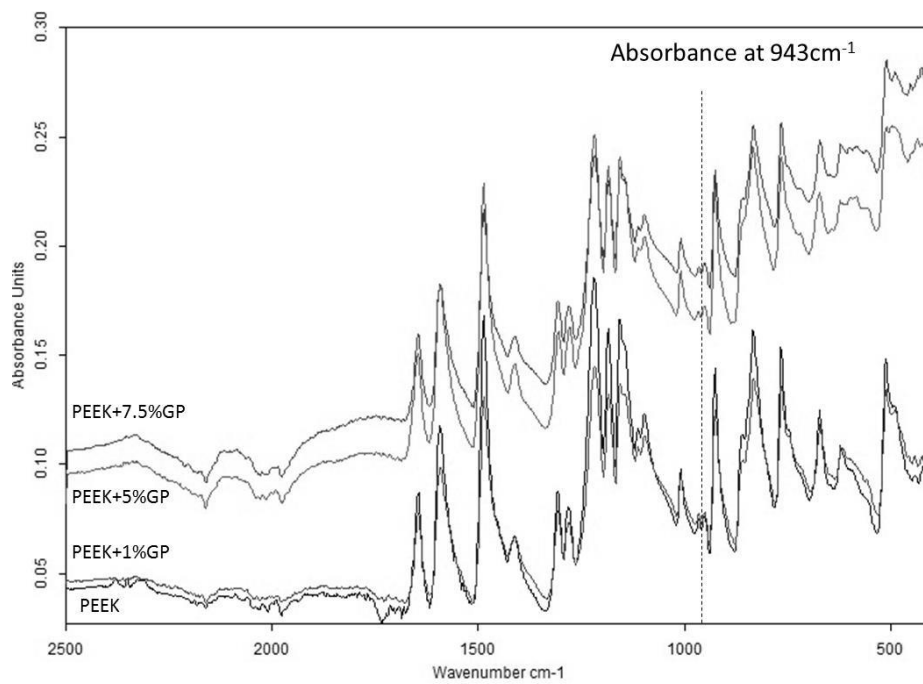
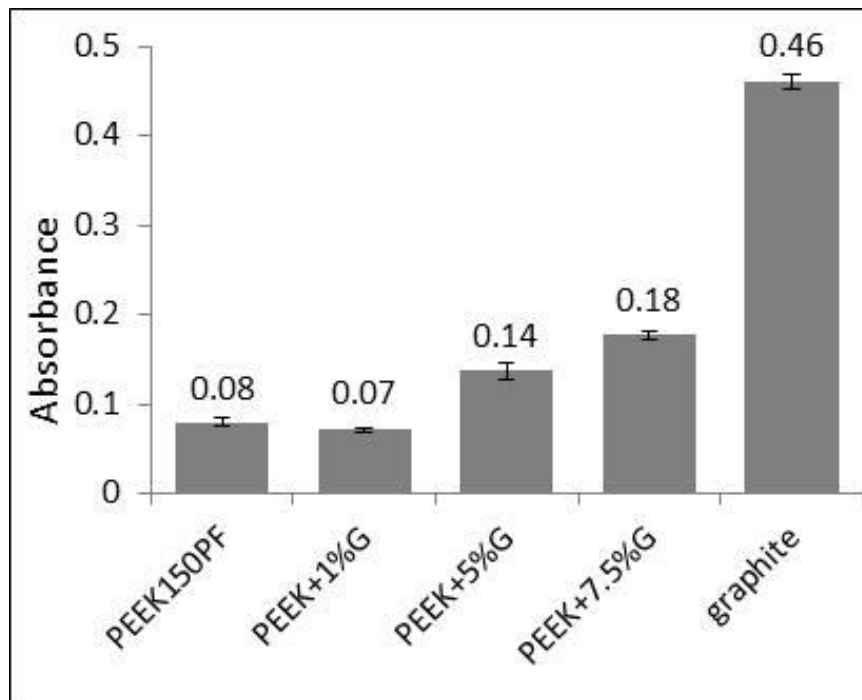
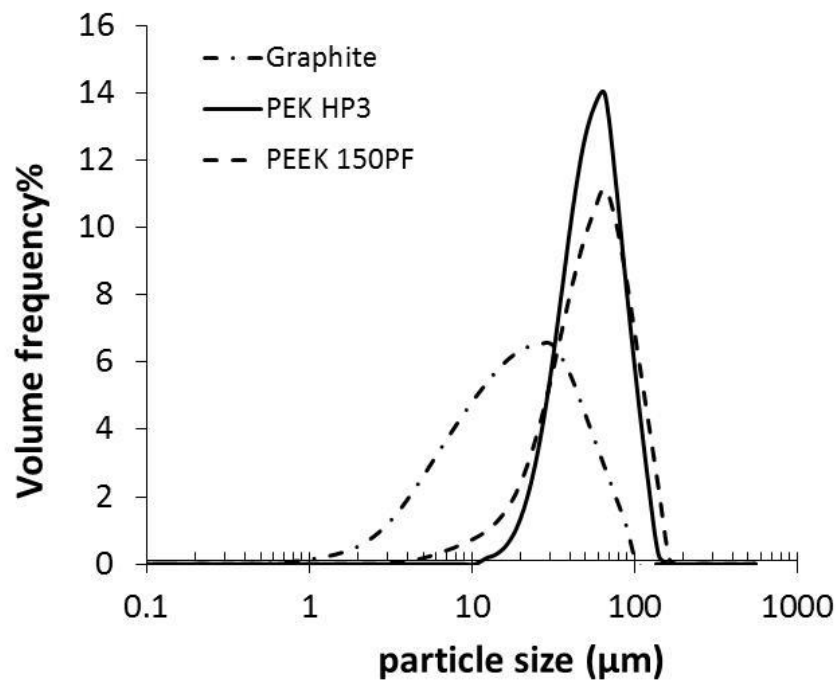


Figure 2: Schematic image showing a typical laser sintered tensile test specimen and the location of a micro-CT sample cut from it.



(a)



(b)

Figure 3: (a) FTIR spectra and absorbance of PEEK and PEEK/GP composite with 1%, 5% and 7.5wt% loadings and pure graphite platelets at  $943\text{cm}^{-1}$  wavenumbers. (b) Particle size distribution of PEK HP3, PEEK 150PF and graphite powders.

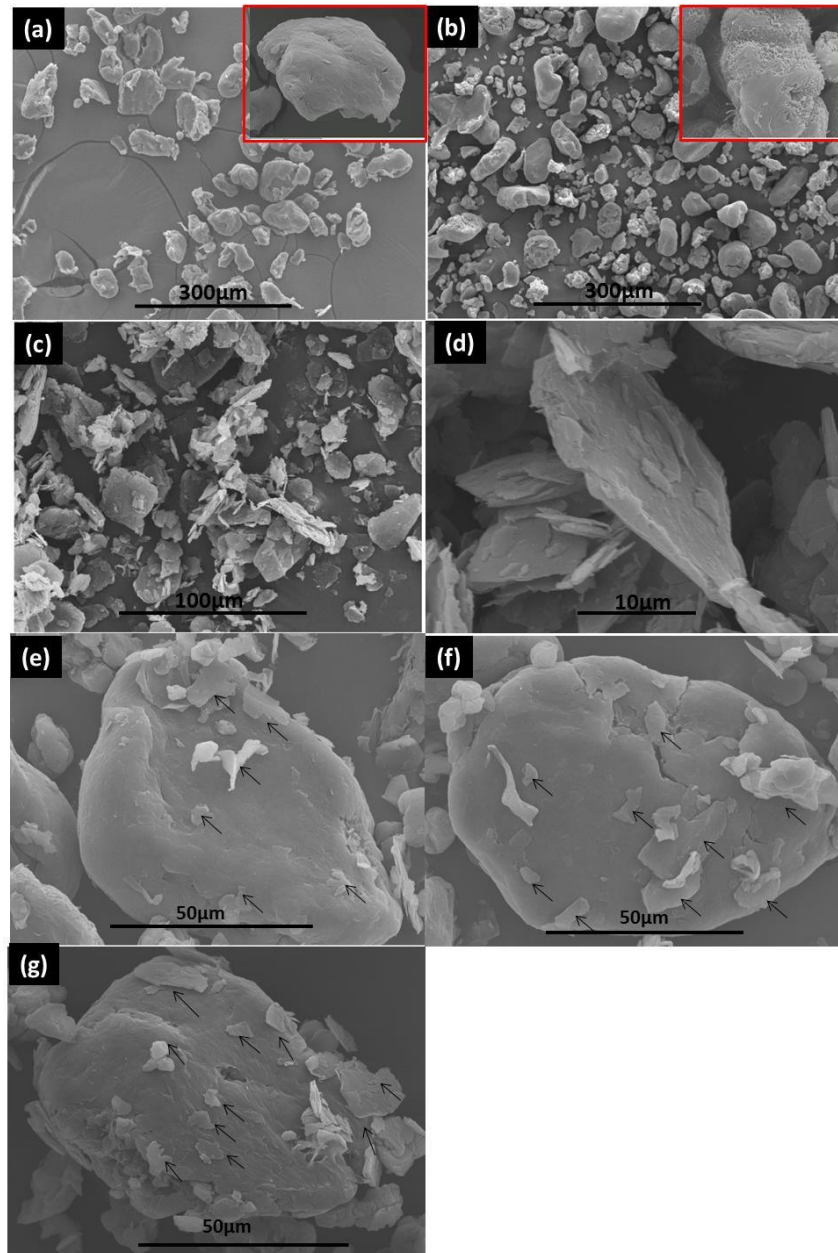


Figure 4: SEM image of (a) PEK powder, (b) PEEK powder, (c) graphite platelets, (d) high magnification image of graphite platelets and (e) (f) (g) the surface of PEEK powder coated with graphite platelets in the dry mixed powder with 1wt%, 5wt% and 7.5wt %GP. High magnification images of PEK and PEEK powder are displayed in the upper right corner of (a) and (b). The PEEK particles (b) have elongated shapes and their surfaces are rougher compared with the commercial PEK grade (a). (c) and (d) show the shape of the graphite flakes. The increased surface roughness leads to increased friction amongst particles which reduces the flowability. The PEEK particles are predominantly coated by the small graphite platelets with sizes of less than 30μm (e)-(g). These graphite platelets could effectively improve the laser absorption and help transfer the heat to the PEEK particles.

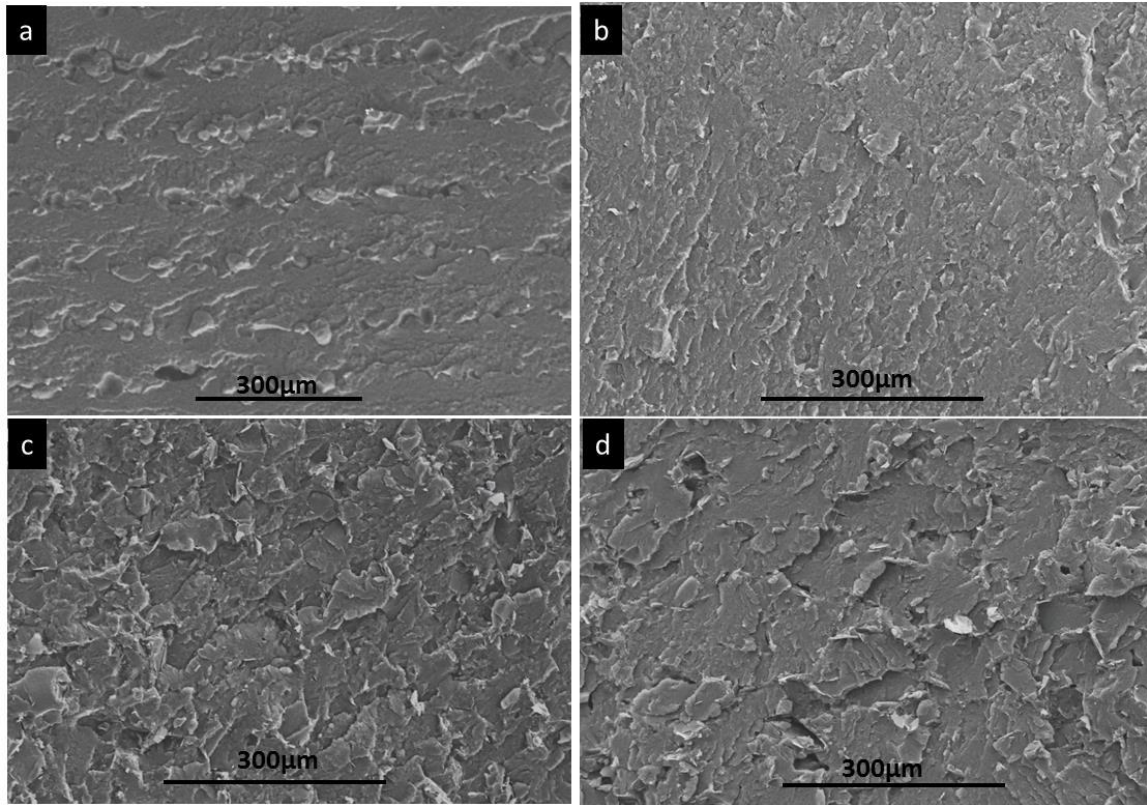


Figure 5: The fracture surface image of laser sintered materials (a) pure PEEK, (b) PEEK/1%GP composite, (c) PEEK/5%GP composite and (d) PEEK/7.5%GP composite. (a) shows the layered microstructure induced by the manufacturing process. The presence of graphite improves the fusion between layers and leads to a more homogeneous structure, as seen in (b), (c) and (d).

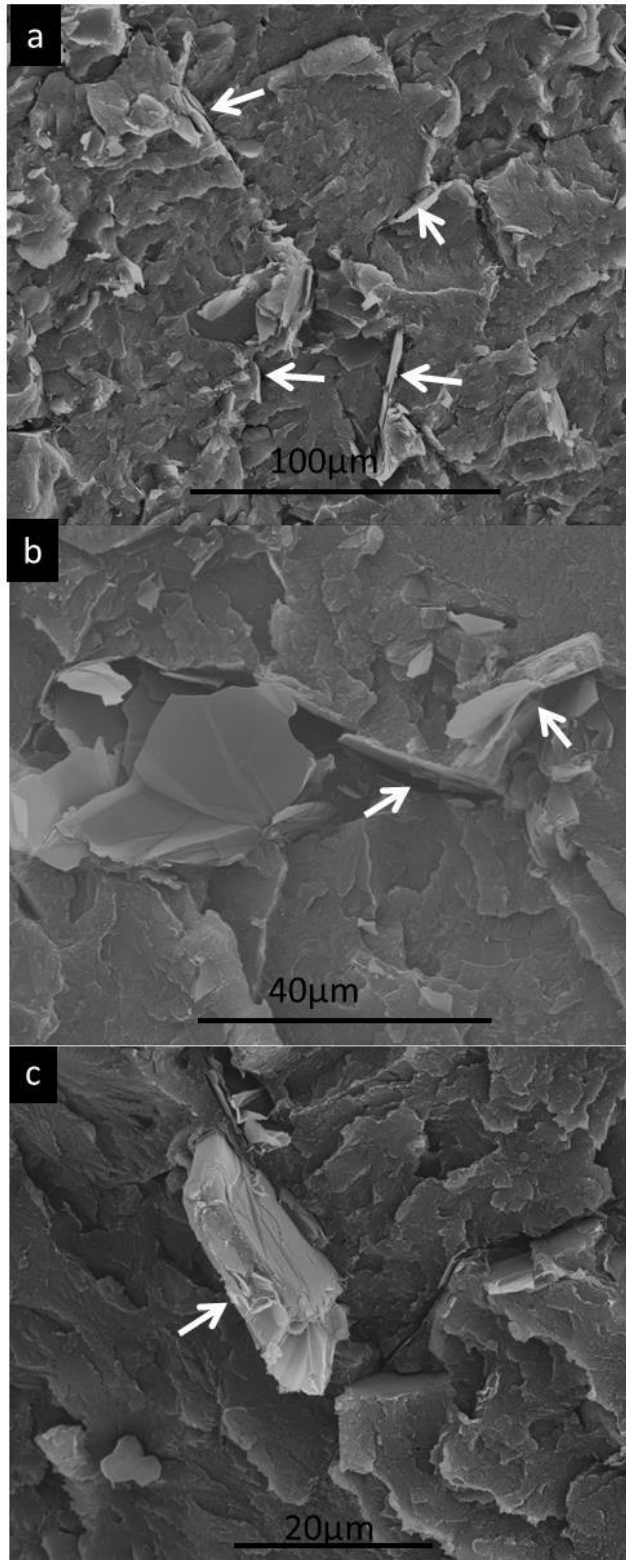
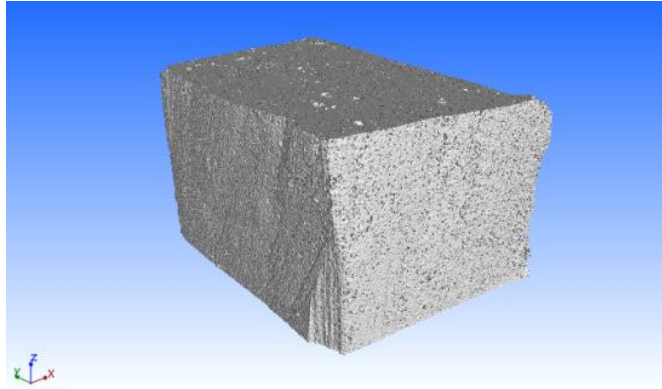
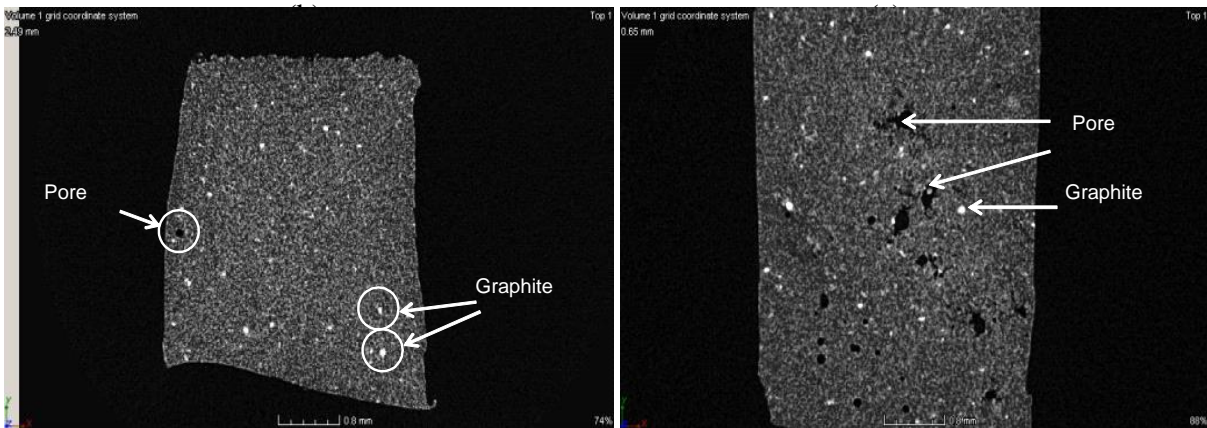
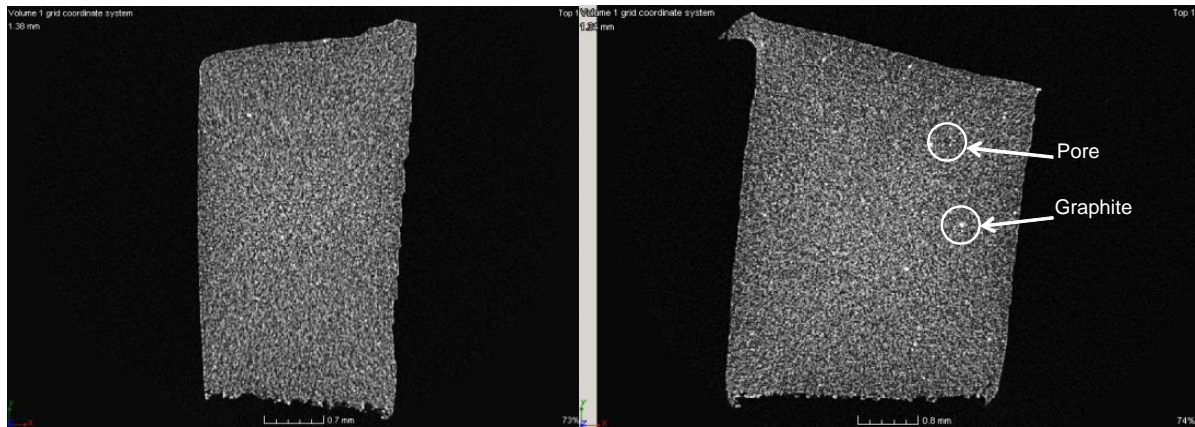


Figure 6: Fracture surface SEM image of PEEK/graphite composites (a), (b) and (c) showing the orientation of graphite platelets within the laser sintered composites at different magnifications. The images reveal the presence of some graphite platelets partially pulled out of the matrix with an out-of-plane orientation.



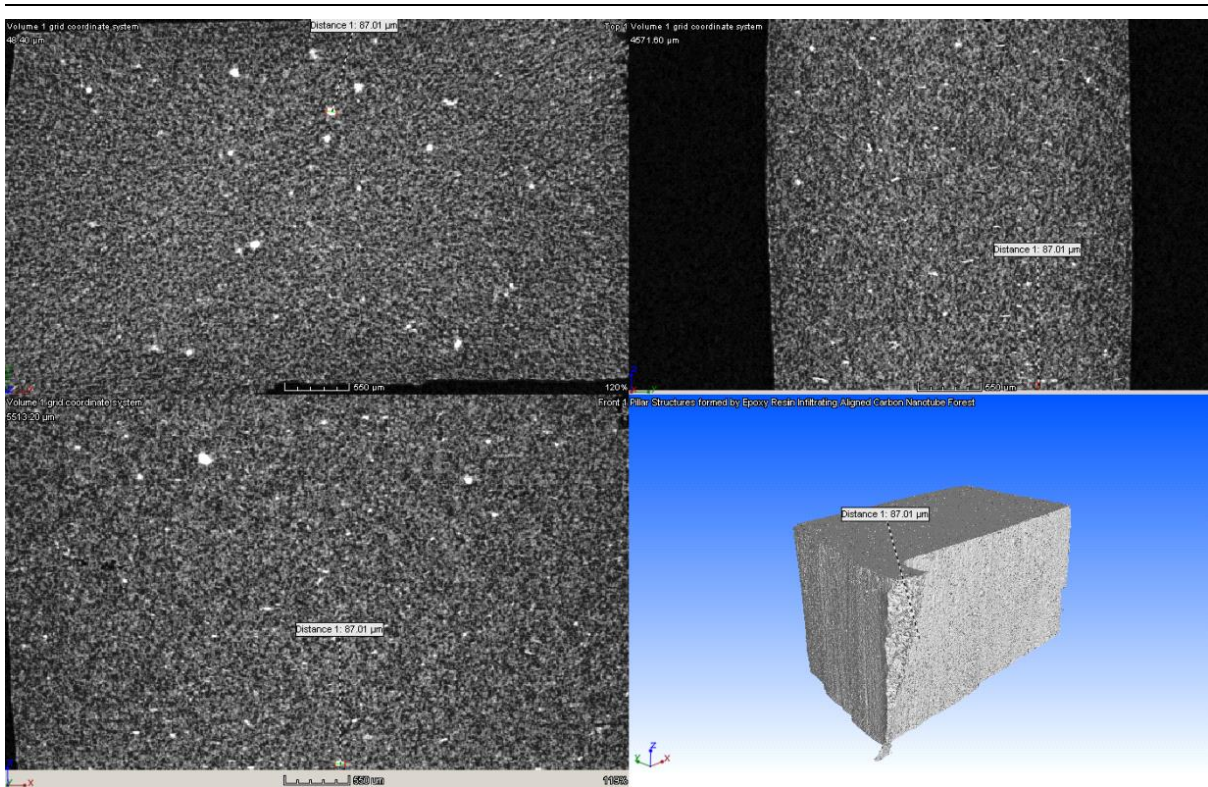
(a)



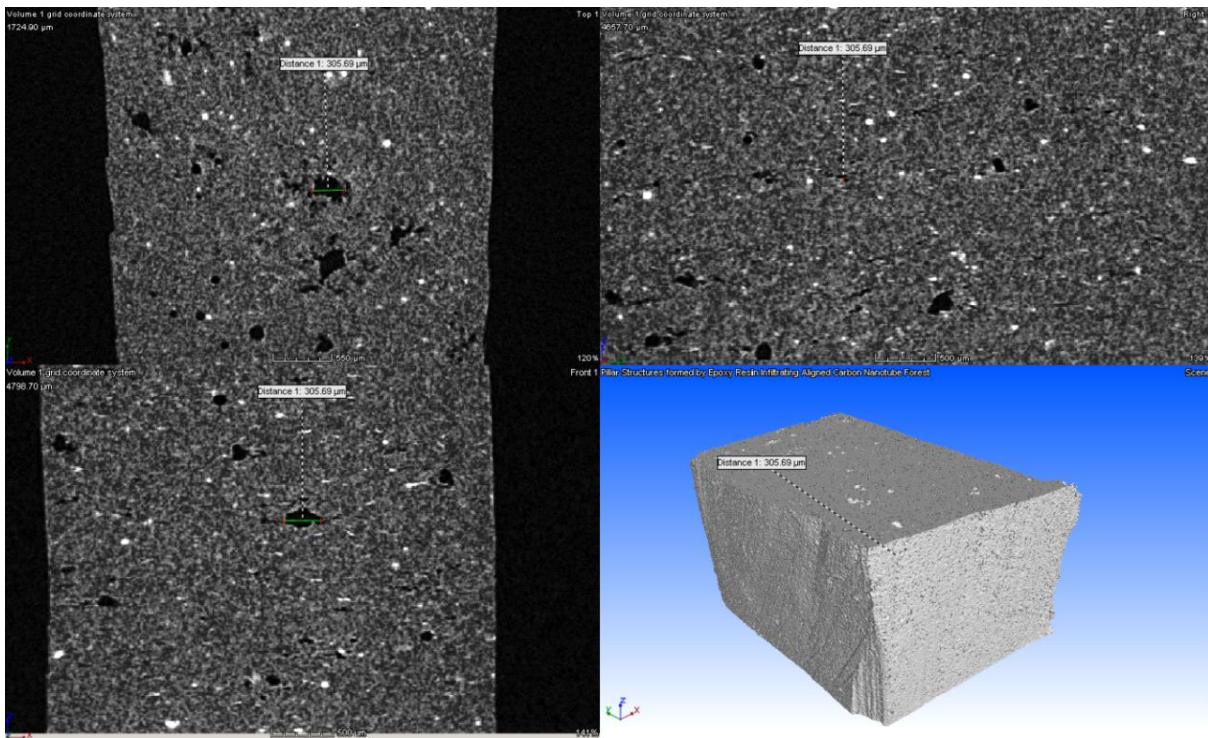
(d)

(e)

Figure 7: (a) Micro-CT 3D image of a PEEK/7.5% GP sample, (b) 2D image in z direction of PEEK sample (c) 2D image in z direction of a PEEK/1% GP sample, (d) 2D image in z direction of a PEEK/5% GP sample, (e) 2D image in z direction of a PEEK/7.5% GP sample.

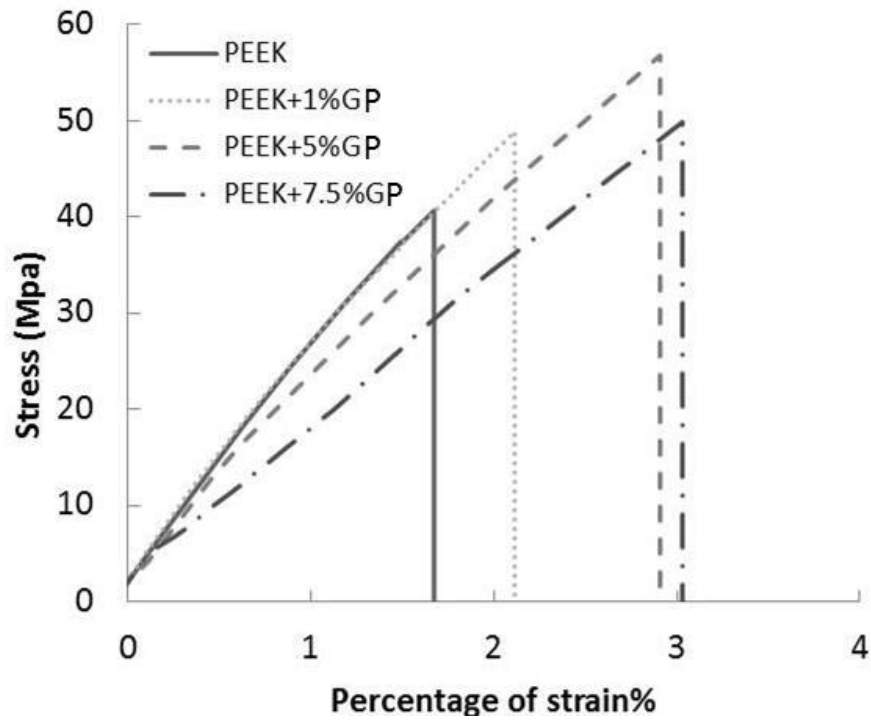


(a)

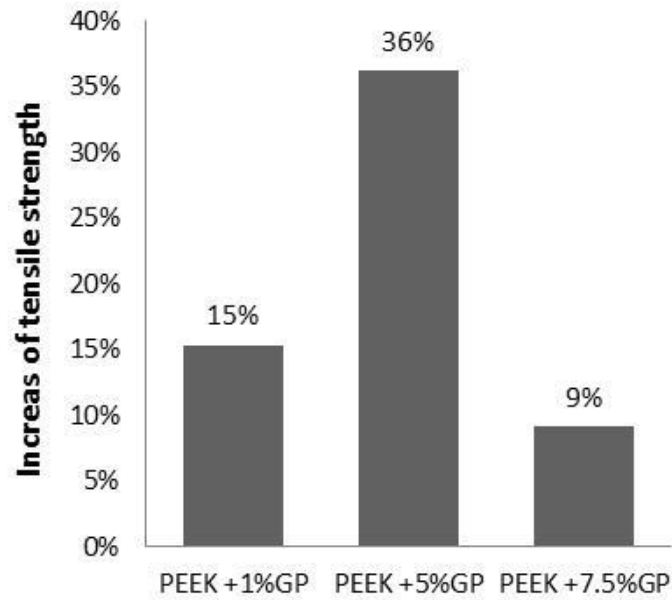


(b)

Figure 8: Micro-CT 3D and 2D images from different directions for PEEK structures with (a) 5% graphite, (b) 7.5% graphite loadings



(a)



(b)

Figure 9: (a) Strain-Stress curve of PEEK and PEEK composites and (b) % increase in tensile strength for composites (with varying percentages of graphite platelets.)

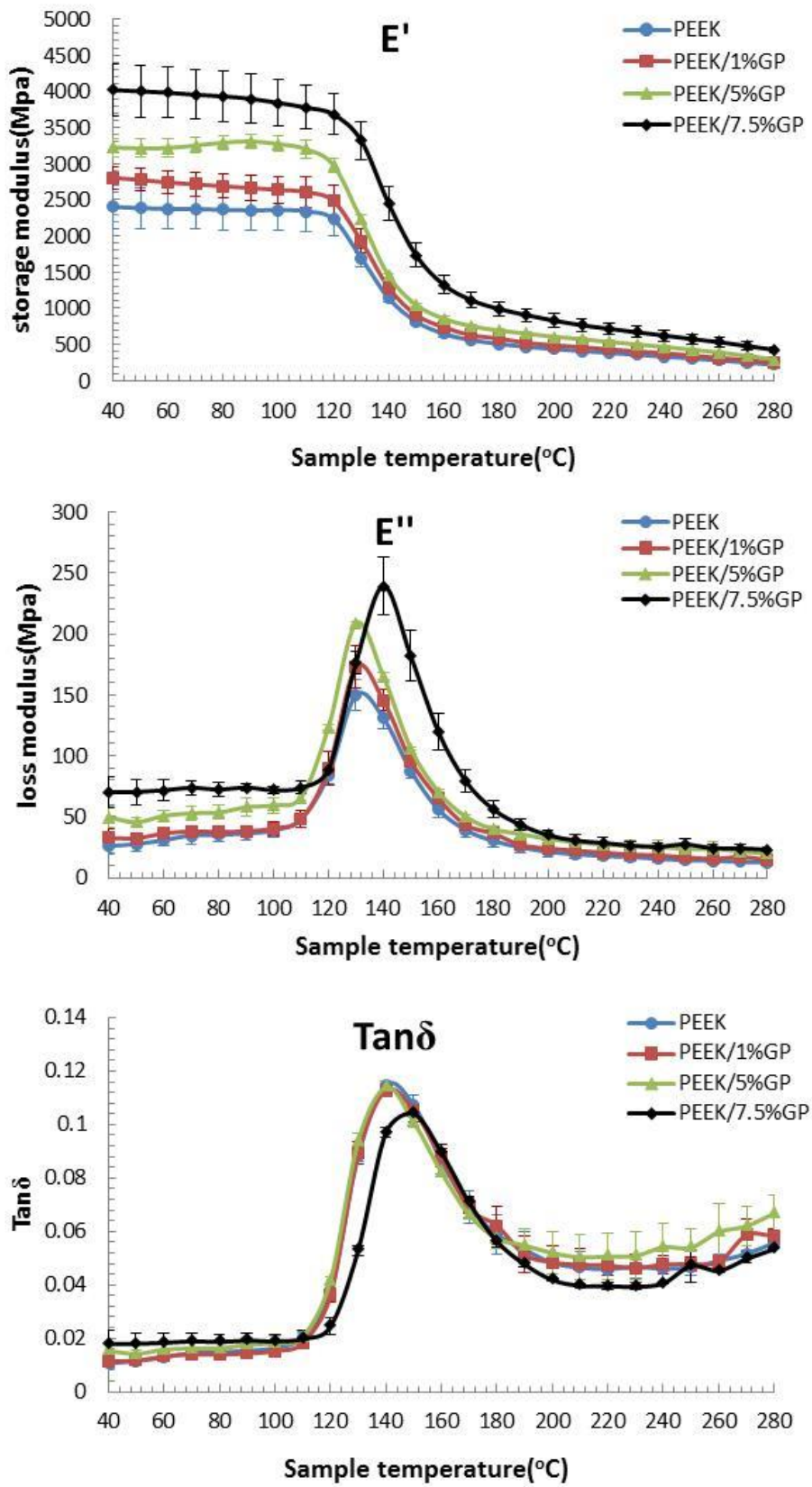


Figure 10: Thermal mechanical behaviour of PEEK and PEEK/GP composites

